Iran Polym J (2013) 22:9–14
DOI 10.1007/s13726-012-0098-y

ORIGINAL PAPER

Magnetic cobalt-zinc ferrite/PVAc nanocomposite: synthesis and characterization

F. S. Mohammad Doulabi · M. Mohsen-Nia

Received: 28 February 2012 / Accepted: 26 September 2012 / Published online: 18 October 2012

Abstract Metal oxide nanoparticles are the subject of current interest because of their unusual optical, electronic, and magnetic properties. In this work, cobalt zinc ferrite ($Co_{0.3}Zn_{0.7}Fe_2O_4$) nanoparticles have been synthesized successfully through redox chemical reaction in aqueous solution. The synthesized $Co_{0.3}Zn_{0.7}Fe_2O_4$ nanoparticles have been used for the preparation of homogenous polyvinyl acetate-based nanocomposite ($Co_{0.3}Zn_{0.7}Fe_2O_4$/PVAc) via in situ emulsion polymerization method. Structural, morphological and magnetic properties of the products were determined and characterized in detail by X-ray powder diffractometry (XRD), Fourier transform infrared spectroscopy (FTIR), scanning electron microscopy (SEM), transmission electron microscopy (TEM) and vibrating sample magnetometer (VSM). The XRD patterns of the $Co_{0.3}Zn_{0.7}Fe_2O_4$ confirmed that the formed nanoparticles are single crystalline. According to TEM micrographs, the synthesized $Co_{0.3}Zn_{0.7}Fe_2O_4$ nanoparticles had nano-needle morphology with an average particle size of 20 nm. The calculated coefficient of variation (CV) of nanoparticles diameters obtained by TEM micrographs was 16.77. The $Co_{0.3}Zn_{0.7}Fe_2O_4$ nanoparticles were dispersed almost uniformly in the polymer matrix as was proved by SEM technique. The magnetic parameters of the samples, such as saturation magnetization (M_s) and coercivity (H_c) were measured, as well. Magnetization measurements indicated that the saturation magnetization of synthesized $Co_{0.3}Zn_{0.7}Fe_2O_4$/PVAc nanocomposites was markedly less than that of $Co_{0.3}Zn_{0.7}Fe_2O_4$ magnetic nanoparticles. However, the nanocompoites exhibited super-paramagnetic behavior at room temperature under an applied magnetic field.

Keywords Magnetic material · Polymer-based nanocomposite · $Co_{0.3}Zn_{0.7}Fe_2O_4$ · PVAc · VSM

F. S. M. Doulabi · M. Mohsen-Nia
Department of Chemistry, University of Kashan, Kashan, Iran

F. S. M. Doulabi
Department of Chemistry, South Tehran Branch, Islamic Azad University, Tehran, Iran

M. Mohsen-Nia (✉)
Division of Chemistry and Chemical Engineering, Caltech, Pasadena, CA, USA
e-mail: moh.moh@cheme.caltech.edu

Introduction

Due to their unique physicochemical properties, magnetic nanoparticles have been intensively studied in recent years. Magnetic nanoparticles are being actively used for different applications, such as magnetic resonance imaging contrast enhancement, detoxification of biological fluids, drug delivery, and cell separation techniques [1]. For different applications, magnetic nanoparticles are used for preparing polymer-based nanocomposites [2, 3]. Polymers and copolymers with a wide variety of compositions, structures, and properties are available, which make them ideal components for use in nanocomposite materials. Main feature of polymeric nanocomposite, in contrast to conventional composites, is due to their enhanced thermal, mechanical and magnetic properties. However, the structure and properties of polymer-based nanocomposites especially magnetic nanocomposites are significantly affected by quantitative and qualitative specifications of nanoparticles as well as local chemistry, chain mobility, chain conformation, and crystallinity of the polymer matrix. Nevertheless, in magnetic polymer-based nanocomposites,

controlled dispersion of magnetic nanoparticles inside the polymer matrix is critical and often challenging. Owing to the non-perfect dispersion of magnetic nanoparticles in the polymer matrix, clusters which are influenced by particle–particle and particle–matrix interactions may be formed. Therefore, to achieve excellent dispersion, the magnetic nanoparticles should be prevented from the formation of larger agglomerates in polymer nanocomposites.

Spinel nanoparticles with general formula "AB_2O_4" ("A" refers to cations in tetrahedral sites and "B" refers to cations in the octahedral positions) have been used in various technological applications. They show various magnetic properties depending on the composition and cation distribution. Various cations can be placed in A and B sites to tune their magnetic properties. Depending on A and B sites cations, spinel nanoparticles can exhibit ferrimagnetic, antiferromagnetic, spin (cluster) glass, and paramagnetic behavior.

Among these materials, nanoscale spinel ferrites (AFe_2O_4) exhibit super-paramagnetic characteristic which is fundamental to biomedical applications such as magnetic contrast resonance imaging (MRI). The fabrication of ferrite nanoparticles has been intensively investigated in recent years due to their unique physical and chemical properties. Introducing of metal ions such as Zn, Co, and Mn into the tetrahedral sites of spinel ferrites offers an opportunity to prepare different grades of magnetic nanoparticles [4].

Physical properties of the Co–Zn spinel ferrites ($Co_xZn_{1-x}Fe_2O_4$) nanoparticles are very sensitive to the amount of metal ions and the method of preparation. Considering the ferrimagnetic, antiferromagnetic, and paramagnetic applicabilities of the Co–Zn ferrites nanoparticles, various synthesis process methods such as coprecipitation, reverse micelle method, sol–gel method, ultrasound irradiation, freeze drying, thermal decomposition of organometallic and coordination compounds, hydrothermal and microwave assisted methods have been used [5–8].

Due to their attractive magnetic and electric properties, synthesis and characterization of various magnetic particles were published in literature in recent years [9–11]. Some of the reported types of nanocomposites are magnetic–metal (Fe_3O_4–Au) [12], magnetic–metallic oxide (Zn, Ni Ferrite–NiO) [13], magnetic–semiconductors (Fe_3O_4–PbS) [14], magnetic–alloy (($Ni_{0.5}Zn_{0.5}$) Fe_2O_4–$FeNi_3$) [15], magnetic–zeolite [16] and magnetic–polymer [17].

In this work, high-purity grade nanosized $Co_{0.3}Zn_{0.7}Fe_2O_4$ particles were synthesized for preparing the stable $Co_{0.3}Zn_{0.7}Fe_2O_4$/PVAc nanocomposite. By considering the simplicity, low cost, and use of an aqueous-based processing system, a convenient coprecipitation method was used for the synthesis of $Co_{0.3}Zn_{0.7}Fe_2O_4$ nanoparticles. $Co_{0.3}Zn_{0.7}Fe_2O_4$/PVAc Nanocomposite was synthesized via an in situ polymerization in emulsion system. The obtained results indicated that magnetic $Co_{0.3}Zn_{0.7}Fe_2O_4$/PVAc nanocomposites combine the advantageous properties of both $Co_{0.3}Zn_{0.7}Fe_2O_4$ and PVAc.

Experimental

Materials

Commercial grade vinyl acetate (VAc, $C_4H_6O_2$) and poly vinyl alcohol (PVA, $(C_2H_4O)_n$, degree of hydrolysis 88 % degrees of polymerization 580, $M_w = 90{,}000$) were supplied from Iran petrochemical Co., Iran and Kuraray Chemical Co., Japan, respectively. Vinyl acetate monomer was distilled under reduced pressure before use. Cobalt chloride hexahydrate ($CoCl_2.6H_2O$), zinc chloride ($ZnCl_2$), iron chloride ($FeCl_3$), oleic acid ($C_{18}H_{34}O_2$), ammonia solution (NH_3), ammonium persulfate (APS) and sodium bicarbonate ($NaHCO_3$) were purchased from Merck, Germany. Sodium lauryl sulfate (SLS 99 %) was supplied by Fluka, Switzerland. All chemicals were used without further purification. Water was distilled after being ion-exchanged.

Preparation of $Co_{0.3}Zn_{0.7}Fe_2O_4$

Nanocrystalline $Co_{0.3}Zn_{0.7}Fe_2O_4$ particles have been synthesized by a chemical coprecipitation method [6]. AR grades of $CoCl_2.6H_2O$, $ZnCl_2$ and $FeCl_3$ were used as precursors. Initially, 1 mmol of $CoCl_2.6H_2O$, 2.3 mmol of $ZnCl_2$ and 6.4 mmol of $FeCl_3$ were dissolved in 100 mL distilled water in a 250 mL glass beaker and homogenized at 65 °C. Then, 25 % ammonia solution was added drop wise with constant stirring and the pH of the solution was maintained at 10. The mixture was then heated at 85 °C for about 1 h. A surfactant coating of oleic acid was made to the individual particles to prevent agglomeration into large aggregates. The precipitate was filtered, washed several times with double distilled water, dried at 75 °C and calcined for 5 h at 750 °C.

Synthesis of $Co_{0.3}Zn_{0.7}Fe_2O_4$/PVAc nanocomposite

$Co_{0.3}Zn_{0.7}Fe_2O_4$/PVAc nanocomposite with nanoparticle loading (3 wt %) was prepared by in situ emulsion polymerization of VAc monomer. In the first step, the synthesized $Co_{0.3}Zn_{0.7}Fe_2O_4$ powder was poured directly into 50 ml of distilled water overnight under vigorous stirring and then was dispersed by ultrasonication at room temperature to prevent aggregation of nanoparticles. Then, the mixture was poured into a three-neck flask containing a solution of 0.1 g of APS and 0.1 g buffer solution of

$NaHCO_3$. A glass reactor was equipped with a reflux condenser, a funnel, a water jacket to maintain a constant temperature (±0.1 °C) and a mechanical stirrer under constant agitation (200–300 rpm). The aqueous emulsified solution containing 2 g PVA and 0.2 g SLS was added to the reaction system. The mixture was stirred at 300 rpm and heated up to 75 °C. Afterward, the monomer was fed into the reactor in separate stream with constant flow rates to maintain the reaction system at 75 °C. Time of feeding was almost 80 min and after monomer addition, the polymerization was carried out under an inert nitrogen atmosphere for 4 h. Afterward, the temperature was maintained at 90 °C for 1 h with constant stirring. The synthesized $Co_{0.3}Zn_{0.7}Fe_2O_4$/PVAc nanocomposite was dried at 70 °C for 24 h under vacuum.

Characterization

Fourier transform infrared (FTIR) spectroscopy was recorded by (Magna 550; Nicolet, USA) in the range of 4000–400 cm^{-1} using KBr pellets. XRD patterns of the samples were collected on a X-ray diffractometer (Philips X'Pert MPD, The Netherlands) with Cu–Kα radiation ($\lambda = 1.54$ Å) at a generator voltage of 40 kV and a generator current of 40 mA. The surface morphology and particle diameters of the synthesized $Co_{0.3}Zn_{0.7}Fe_2O_4$ nanoparticles and $Co_{0.3}Zn_{0.7}Fe_2O_4$/PVAc nanocomposite specimens were investigated using a scanning electron microscope (SEM, Philips, The Netherlands). Prior to SEM examination; the samples were dried at room temperature and coated with a thin layer of gold, using a coating machine (Jeol ion-sputter, JFC-1100, Japan).

Morphology of $Co_{0.3}Zn_{0.7}Fe_2O_4$ nanoparticles was studied using transmission electron microscope (TEM) operating at an accelerating voltage of 120 kV. Samples were prepared as follows: fine power of $Co_{0.3}Zn_{0.7}Fe_2O_4$ nanoparticles were dispersed in ethanol under ultrasonication at 25 °C for 10 min, and then one drop of the dilute suspension of colloid was suspended and evaporated on a carbon-coated copper grid and placed in the Phillips CM-120 TEM (The Netherlands). The magnetic properties, saturation magnetization, coercivity and retentivity of samples were determined from the magnetic moment versus magnetization curves recorded for various samples with the help of a vibrating sample magnetometer (VSM) device, in the Development Center of Kashan University, Iran, under maximum magnetic field of 10 kOe.

Results and discussion

The FTIR spectrum of the synthesized $Co_{0.3}Zn_{0.7}Fe_2O_4$ nanoparticles and $Co_{0.3}Zn_{0.7}Fe_2O_4$/PVAc nanocomposite are shown in Fig. 1. Spectrum (a) in Fig. 1 shows the characteristic peaks of tetrahedral and octahedral Fe–O stretching bands at 558 and 420 cm^{-1}, respectively. In addition to these vibrational modes, a broad hump due to water symmetric stretching and antisymmetric stretching with maxima at about 3435 cm^{-1} and the bending mode of water at 1630 cm^{-1} are observed in these spectra. In ferrites, the metal ions are situated in two different sub-lattices designated tetrahedral (A sites) and octahedral (B sites) according to the geometrical configuration of the oxygen nearest neighbors.

In the spectrum of the $Co_{0.3}Zn_{0.7}Fe_2O_4$/PVAc nanocomposite as shown in Fig. 1, spectrum (b), the peak observed at 3440 cm^{-1} can be attributed to the hydroxyl stretching vibration, the peak at 2941 cm^{-1} can likely be assigned to the C–H stretching vibration, and the peak found at

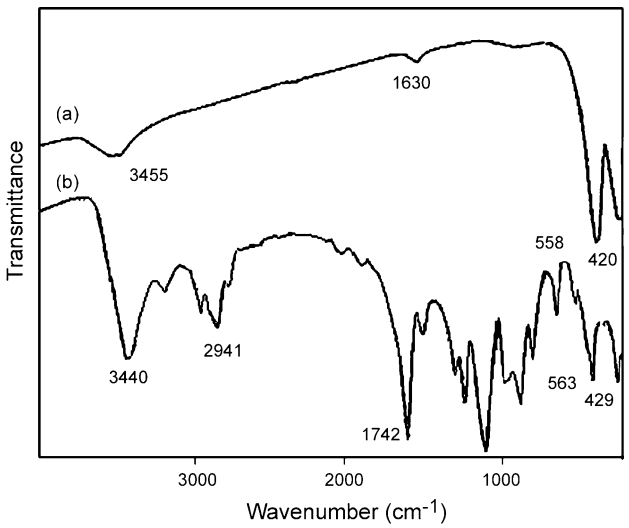

Fig. 1 FTIR Spectra of (**a**) $Co_{0.3}Zn_{0.7}Fe_2O_4$ and (**b**) $Co_{0.3}Zn_{0.7}Fe_2O_4$/PVAc nanocomposite

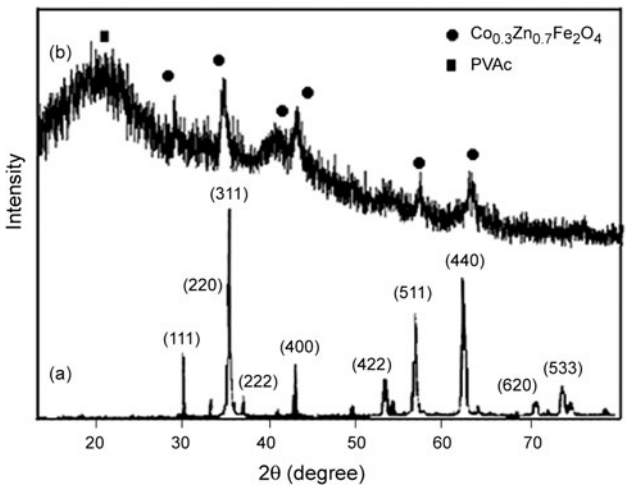

Fig. 2 XRD patterns of (**a**) $Co_{0.3}Zn_{0.7}Fe_2O_4$ and (**b**) $Co_{0.3}Zn_{0.7}Fe_2O_4$/PVAc nanocomposite

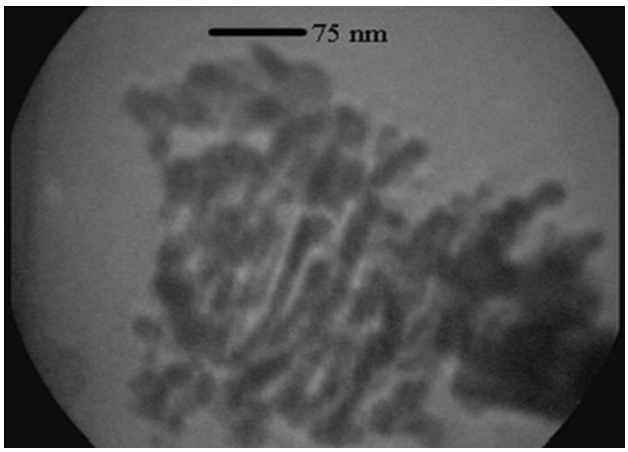

Fig. 3 TEM image of the $Co_{0.3}Zn_{0.7}Fe_2O_4$ nanoparticles

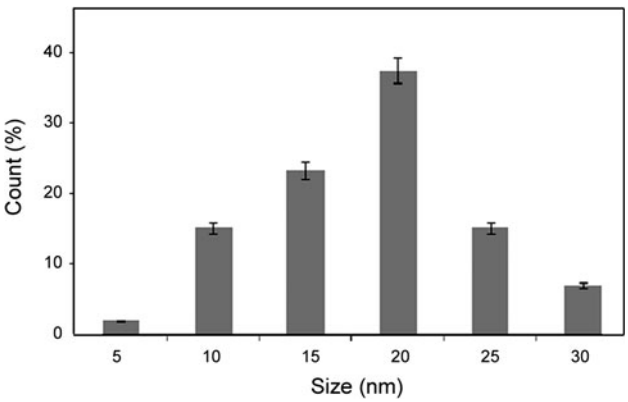

Fig. 4 Particle size distribution of $Co_{0.3}Zn_{0.7}Fe_2O_4$ nanoparticles

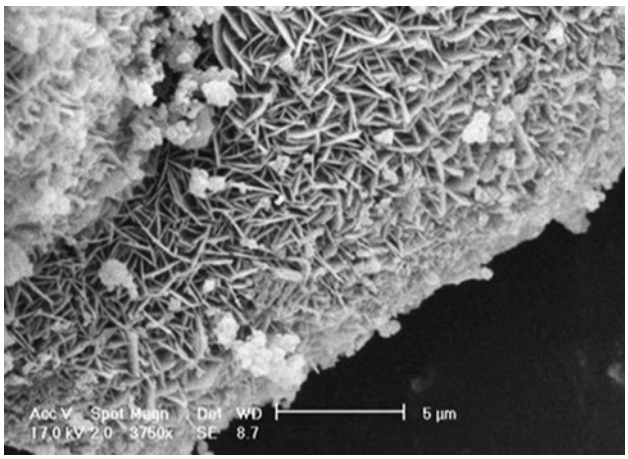

Fig. 5 SEM micrograph of $Co_{0.3}Zn_{0.7}Fe_2O_4$ nanoparticles

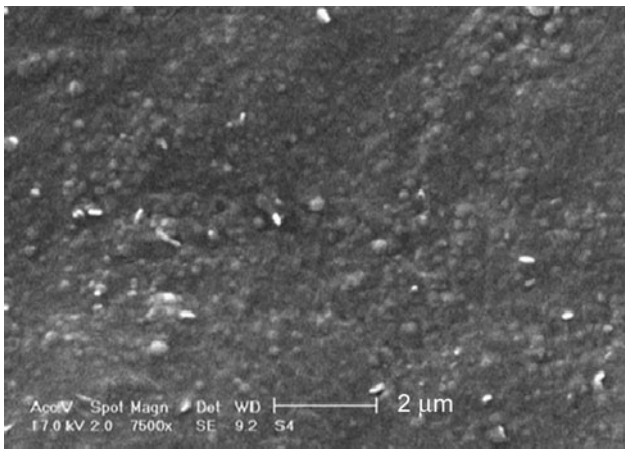

Fig. 6 SEM micrograph of $Co_{0.3}Zn_{0.7}Fe_2O_4$/PVAc nanocomposite

1742 cm^{-1} originates with the C=O stretching vibration. The peak at 1439 cm^{-1} comes from the C–H bending vibration, the peaks observed at 1242 and 1123 cm^{-1} are associated with the C–O–C symmetrical stretching vibrations [18]. The absorption peaks at 563 and 429 cm^{-1} may be attributed to the intrinsic vibration of the tetrahedral and octahedral sites in the $Co_{0.3}Zn_{0.7}Fe_2O_4$ particles [19].

Pattern (a) in Fig. 2 shows the XRD powder pattern of the nanoparticles. All XRD peaks are corresponds with the JCPDS cards no. 89-1012 ($ZnFe_2O_4$) and 22-1086 ($CoFe_2O_4$). Analysis of the diffraction pattern using (111), (220), (311), (222) (400), (422), (511), (440), (620), (533) and (622) reflection planes confirmed the formation of spinel structure of the $Co_{0.3}Zn_{0.7}Fe_2O_4$. The lattice constant (a) for each peak of $Co_{0.3}Zn_{0.7}Fe_2O_4$ can be calculated using the following equation:

$$a = d\left(h^2 + k^2 + l^2\right)^{1/2} \quad (1)$$

where, d is the spacing of (hkl) crystal planes. The calculated lattice constant was 8.391 Å for (111) plane. The (311) peak was chosen for calculating the average particle size by using the Debye–Sherrer equation as follows:

$$D = k\lambda/\beta\cos\theta \quad (2)$$

where, λ is the wavelength of the radiation, β is the full-width at half-maxima (FWHM), θ is the diffraction angle and D is the particle size of the sample (nm). The calculated average particle size of $Co_{0.3}Zn_{0.7}Fe_2O_4$ nanaoparticles was about 10.9 nm.

XRD pattern of the $Co_{0.3}Zn_{0.7}Fe_2O_4$/PVAc nanocomposite is shown as pattern (b) in Fig. 2. According to this pattern, the characteristic peaks of both PVAc and $Co_{0.3}Zn_{0.7}Fe_2O_4$ confirm the formation of the $Co_{0.3}Zn_{0.7}Fe_2O_4$/PVAc nanocomposite. Furthermore, diffraction peaks of $Co_{0.3}Zn_{0.7}Fe_2O_4$/PVAc nanocomposite compared to those of $Co_{0.3}Zn_{0.7}Fe_2O_4$ nanoparticles were broader due to the polymer matrix's restriction on the nanoparticles [20].

TEM micrograph of synthesized $Co_{0.3}Zn_{0.7}Fe_2O_4$ nanoparticles is given in Fig. 3 and their particle size

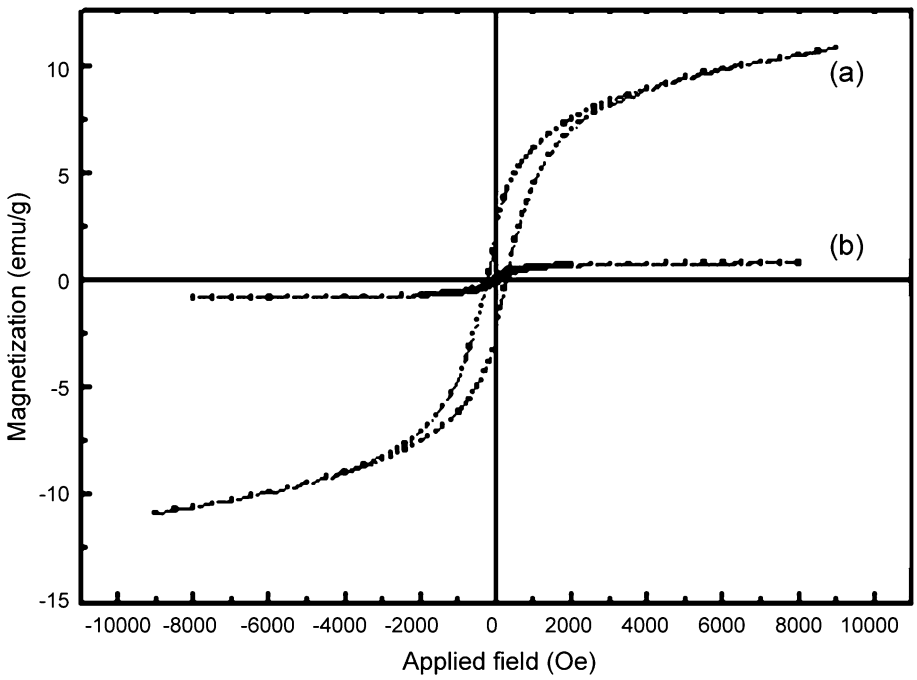

Fig. 7 Hysteresis loops for: (**a**) $Co_{0.3}Zn_{0.7}Fe_2O_4$ nanoparticles and (**b**) $Co_{0.3}Zn_{0.7}Fe_2O_4$/PVAc nanocomposite

Table 1 Values of M_s and H_c for $Co_{0.3}Zn_{0.7}Fe_2O_4$ nanoparticles and $Co_{0.3}Zn_{0.7}Fe_2O_4$/PVAc nanocomposite

Samples	M_s (emu/g)	H_c (Oe)
$Co_{0.3}Zn_{0.7}Fe_2O_4$	10.82	742.6
$Co_{0.3}Zn_{0.7}Fe_2O_4$/PVAc	0.82	12.24

distribution is presented in Fig. 4. Generally, the particles have nano-needle morphology and their sizes vary from 5 to 30 nm. The average size of the $Co_{0.3}Zn_{0.7}Fe_2O_4$ nanoparticles was 20 nm. The coefficient of variation (CV) of particle diameter was defined using the following equation by counting individual particles from TEM microphotograph:

$$CV = \frac{\left(\sum d_i - (\sum n_i d_i / \sum n_i)^2 \Big/ \sum n_i\right)^{1/2}}{(\sum n_i d_i / \sum n_i)} \times 100 \qquad (3)$$

where, n_i is the number of particles with d_i diameter. The calculated CV was 16.77 from TEM micrograph.

Figure 5 shows the SEM micrograph of the $Co_{0.3}Zn_{0.7}Fe_2O_4$ nanoparticles sample. It provides more structural information about the three-dimensional morphology of the product. According to this figure, the synthesized $Co_{0.3}Zn_{0.7}Fe_2O_4$ nano-needle particles have very narrow diameter distribution.

Figure 6 shows the SEM micrograph of $Co_{0.3}Zn_{0.7}Fe_2O_4$/PVAc nanocomposite. According to this figure, the nanosized $Co_{0.3}Zn_{0.7}Fe_2O_4$ particles were dispersed almost uniformly in the *PVAc* matrix. The average particle size of the $Co_{0.3}Zn_{0.7}Fe_2O_4$/PVAc nanocomposite is about 150–200 nm.

Magnetic property of the as-prepared $Co_{0.3}Zn_{0.7}Fe_2O_4$ nanoparticle was investigated with a vibrating sample magnetometer (VSM) at room temperature. The magnetic hysteresis loop of $Co_{0.3}Zn_{0.7}Fe_2O_4$ nanaoparticles is shown in Fig. 7, loop (a). The obtained magnetic parameters of the samples, such as saturation magnetization (M_s) and coercivity (H_c) are given in Table 1. According to the obtained results, the M_s value of $Co_{0.3}Zn_{0.7}Fe_2O_4$ nanoparticles was 10.82 emu/g. Small value of M_s may be due to the oleic acid and formation of a surface layer on $Co_{0.3}Zn_{0.7}Fe_2O_4$ nanoparticles in which magnetic moments do not contribute to the magnetization in the applied field.

For ferromagnetic spinels such as $Co_xZn_{1-x}Fe_2O_4$, the changes in magnetic properties such as M_s and H_c are related to the influence of the cationic stoichiometry and their occupancy in the specific sites. It was shown that for $x < 0.5$, the magnetization at room temperature shows approximately linear applied field dependence with small s-shaped behavior [21].

Magnetic hysteresis loop of $Co_{0.3}Zn_{0.7}Fe_2O_4$/PVAc nanocomposite is shown in Fig. 7, loop (b). Saturation magnetization of the $Co_{0.3}Zn_{0.7}Fe_2O_4$/PVAc nanocomposite depends mainly on the volume fraction of magnetic $Co_{0.3}Zn_{0.7}Fe_2O_4$ nanoparticles. However, due to the non-magnetic PVAc coating contribution and its important role in isolating the magnetic $Co_{0.3}Zn_{0.7}Fe_2O_4$ nanoparticles, the M_s of the synthesized $Co_{0.3}Zn_{0.7}Fe_2O_4$/PVAc nanocomposite is much lower than that for $Co_{0.3}Zn_{0.7}Fe_2O_4$ nanoparticles. In addition, the demagnetic effect of *PVAc* may reduce the M_s of the $Co_{0.3}Zn_{0.7}Fe_2O_4$/PVAc nanocomposite. Therefore, the magnetization of the $Co_{0.3}Zn_{0.7}Fe_2O_4$/PVAc

nanocomposites was lower than that of the pure $Co_{0.3}Zn_{0.7}Fe_2O_4$ nanoparticles. According to Table 1, the value of M_s for the synthesized $Co_{0.3}Zn_{0.7}Fe_2O_4$/PVAc nanocomposite was significantly lower compared to that of $Co_{0.3}Zn_{0.7}Fe_2O_4$ nanoparticles.

Conclusion

Considering the extra advantages that could be obtained with combined properties of the inorganic materials (mechanical strength, magnetic and thermal stability) and the organic polymers (flexibility, dielectric, ductility and processability), we first prepared $Co_{0.3}Zn_{0.7}Fe_2O_4$ nanoparticles via a redox chemical reaction in aqueous solution. Then, the synthesized $Co_{0.3}Zn_{0.7}Fe_2O_4$ nanoparticles have been used for preparation of homogenous $Co_{0.3}Zn_{0.7}Fe_2O_4$/PVAc nanocomposite. The synthesized $Co_{0.3}Zn_{0.7}Fe_2O_4$ nanoparticles and $Co_{0.3}Zn_{0.7}Fe_2O_4$/PVAc nanocomposite have been analyzed using FTIR, XRD, TEM, SEM and VSM techniques. The average particle size and calculated CV of particle diameter of $Co_{0.3}Zn_{0.7}Fe_2O_4$ nanoparticles were obtained 20 nm and 16.77, respectively, from the TEM micrograph. The results obtained from XRD indicated the formation of a $Co_{0.3}Zn_{0.7}Fe_2O_4$/PVAc nanocomposite. Due to the non-magnetic PVAc coating contribution, the M_s of the synthesized $Co_{0.3}Zn_{0.7}Fe_2O_4$/PVAc nanocomposite was much lower than that for the $Co_{0.3}Zn_{0.7}Fe_2O_4$ magnetic nanoparticles. However, the synthesized $Co_{0.3}Zn_{0.7}Fe_2O_4$/PVAc nanocomposite presented super-paramagnetic properties. From the magnetic hysteresis loops at room temperature, M_s and H_c of the $Co_{0.3}Zn_{0.7}Fe_2O_4$/PVAc nanocomposite were obtained 10.82 emu/g and 12.24 Oe, respectively. Although, the $Co_{0.3}Zn_{0.7}Fe_2O_4$ nanoparticles were dispersed almost uniformly in the polymer matrix as shown in SEM images, the nonzero coercivity value (i.e., 12.24 Oe) probably occur because a small fraction of the particles aggregate to form clusters larger than the super-paramagnetic limit. In general, according to the obtained results, it has been found that in situ emulsion polymerization used here is a suitable method to disperse the $Co_{0.3}Zn_{0.7}Fe_2O_4$ magnetic nanoparticles in *PVAc* polymer matrix for preparation of the stable magnetic $Co_{0.3}Zn_{0.7}Fe_2O_4$/PVAc nanocomposites.

References

1. Yusoff AN, Abdullah MH (2004) Microwave electromagnetic and absorption properties of some Li -Zn ferrites. J Magn Magn Mater 269:271–280
2. Mohsen-Nia M, Seyed Mohammad Doulabi F (2012) Preparation and Characterization of $CoFe_2O_4$/Poly Vinyl Acetate Nanocomposite. Polym Plast Technol Eng 51(11):1122–1126
3. Stefanescua M, Stoia M, Caizer C, Stefanescu O (2009) Preparation of $(Ni_{0.65}Zn_{0.35}Fe_2O_4)_x/(100 - x)SiO_2$ nanocomposite powders by a modified sol–gel method. Mater Chem Phys 113:342–348
4. Yan W, Jiang W, Zhang Q, Li Y, Wang H (2010) Structure and magnetic properties of nickel–zinc ferrite microspheres synthesized by solvothermal method. Mater Sci Eng, B 171:144–148
5. Thakur S, Katyal SC, Singh M (2009) Structural and magnetic properties of nano nickel–zinc ferrite synthesized by reverse micelle technique. J Magn Magn Mater 321:1–7
6. Popplewell J, Sakhnini L (1995) The dependence of the physical and magnetic properties of magnetic fluids on particle size. J Magn Magn Mater 149:72–78
7. Calero-DdelC VL, Rinaldi C (2007) Synthesis and magnetic characterization of cobalt-substituted ferrite ($Co_xFe_{3-x}O_4$) nanoparticles. J Magn Magn Mater 314:60–67
8. Pradeep A, Priyadharsini P, Chandrasekaran G (2008) Sol–gel route of synthesis of nanoparticles of $MgFe_2O_4$ and XRD, FTIR and VSM study. J Magn Magn Mater 320:2774–2779
9. Ni SB, Lin SM, Pan QT, Yang F, Huang K, He D (2009) Hydrothermal synthesis and microwave absorption properties of Fe_3O_4 nanocrystals. J Phys D Appl Phys 42:55004–55008
10. Pan ZW, Dai ZR, Wang ZL (2001) Nanobelts of semiconducting oxides. Science 291:1947–1949
11. Mohsen-Nia M, Mohammad Doulabi FS (2011) Synthesis and characterization of poly vinyl acetate/montmorillonite nanocomposite by in situ emulsion polymerization technique. Polym Bull 66(19):1255–1265
12. Wang L, Luo J, Fan Q, Suzuki M, Suzuki IS, Engelhard MH, Lin Y, Kim N, Wang JQ, Zhong CJ (2005) Monodispersed core – shell Fe_3O_4@Au nanoparticles. J Phys Chem B 109:21593–21601
13. Vučinić-Vasić M, Antic B, Kremenović A, Nikolic AS, Stoiljkovic M, Bibic N, Spasojevic V, Colomban Ph (2006) Zn, Ni ferrite/NiO nanocomposite powder obtained from acetylacetonato complexes. Nanotechnology 17(19):4877–4884
14. Shi W, Zeng H, Sahoo Y, Ohulchansky TY, Ding Y, Wang ZL, Swihart M, Prasad PN (2006) A general approach to binary and ternary hybrid nanocrystals. Nano Lett 6:875–881
15. Shahane GS, Kumar A, Arora M, Pant RP, Lal K (2010) Synthesis and characterization of Ni–Zn ferrite nanoparticles. J Magn Magn Mater 322:1015–1019
16. Nedić B, Dondur V, Kremenović A, Dimitrijević R, Antić B, Blanuša J, Vasiljević-Radović D, Stoiljković M (2007) Yb^{3+} doped dyphillosilicates prepared by thermaly induced phase transformation of zeolites. Russ J Phys Chem 81:1413–1417
17. Božanić DK, Djoković V, Blanuša J, Nair PS, Georges MK, Radhakrishnan T (2007) Preparation and properties of nano-sized Ag and Ag_2S particles in biopolymer matrix. Eur Phys J E 22:51–59
18. Zhao M, Zhou Y, Bruening ML, Bergbreiter DE, Crooks RM (1997) Inhibition of Electrochemical Reactions at Gold Surfaces by Grafted, Highly Fluorinated, Hyperbranched Polymer Films. Langmuir 13(6):1388–1391
19. Liu H, Xu F, Li L, Wang Y, Qiu H (2009) A novel $CoFe_2O_4$/polyacrylate nanocomposite prepared via an in situ polymerization in emulsion system. Reac Funct Polym 69:43–47
20. Li L, Jiang J, Xu F (2006) Novel polyaniline-$LiNi_{0.5}La_{0.02}Fe_{1.98}O_4$ nanocomposites prepared via an in situ polymerization. Eur Polym J 42:2221–2227
21. Gözüak F, Köseoğlu Y, Baykal A, Kavas H (2009) Synthesis and characterization of $Co_xZn_{1-x}Fe_2O_4$ magnetic nanoparticles via a PEG-assisted route. J Magn Magn Mater 321:2170–2177